European Journal of Pharmaceutics and Biopharmaceutics 188 (2023) 26–32

Contents lists available at ScienceDirect

European Journal of Pharmaceutics and Biopharmaceutics

journal homepage: www.elsevier.com/locate/ejpb

Research paper

# *In vitro-in vivo* relationship for amorphous solid dispersions using a double membrane dissolution-permeation setup

Jacob Rune Jørgensen [a], Wolfgang Mohr [b], Matthias Rischer [b], Andreas Sauer [c], Shilpa Mistry [d], Thomas Rades [a,*], Anette Müllertz [a,e]

[a] Department of Pharmacy, Faculty of Health and Medical Sciences, University of Copenhagen, Universitetsparken 2, 2100 Copenhagen, Denmark
[b] Losan Pharma GmbH, Otto-Hahn-Str. 13, 79395 Neuenburg, Germany
[c] SE Tylose GmbH & Co. KG, Kasteler Str. 45, 65203 Wiesbaden, Germany
[d] Harke Pharma GmbH, Xantener Str. 1, 45479 Mülheim a. d. Ruhr, Germany
[e] Bioneer:FARMA, Department of Pharmacy, University of Copenhagen, Universitetsparken 2, 2100 Copenhagen, Denmark

ARTICLE INFO

*Keywords:*
Efavirenz
vacuum compression molding (VCM)
parallel artificial membrane permeability assay (PAMPA)

ABSTRACT

The use of amorphous solid dispersions (ASDs) is one commonly applied formulation strategy to improve the oral bioavailability of poorly water-soluble drugs by overcoming dissolution rate and/or solubility limitations. While bioavailability enhancement of ASDs is well documented, it has often been a challenge to establish a predictive model describing *in vitro-in vivo* relationship (IVIVR). In this study, it is hypothesized that drug absorption might be overestimated by *in vitro* dissolution-permeation (D/P)-setups, when drug in suspension has the possibility of directly interacting with the permeation barrier. This is supported by the overprediction of drug absorption from neat crystalline efavirenz compared to four ASDs in a D/P-setup based on the parallel artificial membrane permeability assay (PAMPA). However, linear IVIVR ($R^2 = 0.97$) is established in a modified D/P-setup in which the addition of a hydrophilic PVDF-filter acts as a physical boundary between the donor compartment and the PAMPA-membrane. Based on microscopic visualization, the improved predictability of the modified D/P-setup is due to the avoidance of direct dissolution of drug particles in the lipid components of the PAMPA-membrane. In general, this principle might aid in providing a more reliable evaluation of formulations of poorly water-soluble drugs before initiating animal models.

## 1. Introduction

Low aqueous solubility of drug candidates is an ongoing challenge in pharmaceutical development with estimations of 70–90% of low molecular weight pipeline compounds being classified as poorly water-soluble [1]. As a result, several solubility enhancing principles have been investigated over the years, e.g. recrystallization into a metastable polymorphic form, amorphization, salt formation, nanosizing and the use of complexing agents and lipid-based formulations. Depending on the molecular structure and/or the physicochemical properties of the poorly water-soluble drug candidate of interest, one might narrow the list of solubility enhancing strategies down to a few suitable options [2]. For example, without a functional group for salt formation, the rational formulation principle could be based on the melting point and/or lipophilicity thus pointing in the direction of either a lipid-based or an amorphous formulation for "grease ball" and "brick dust" molecules, respectively. Yet, in the absence of a gold standard approach to fit all poorly water-soluble drugs, there might be more than one suitable strategy for a specific drug of interest. Consequently, some drugs have been marketed as both lipid-based formulations and amorphous solid dispersions (ASDs) as is the case for fenofibrate, ritonavir and efavirenz (EFV) [3,4]. Irrespective of the principle, the common aim of such enabling formulations is to bring the drug in solution above its equilibrium solubility at the site of absorption. For ASDs, this is achieved by having the drug molecularly dispersed in a polymer matrix. As the matrix dissolves, drug is liberated from the formulation and can thus go in solution without having to overcome the high lattice energy of its crystalline counterpart. Dissolution of an ASD can thus potentially lead to drug supersaturation in the gastrointestinal fluids and thereby increase absorption by generating a steeper concentration gradient across

* Corresponding author at: Department of Pharmacy, Faculty of Health and Medical Sciences, University of Copenhagen, Universitetsparken 2, 2100 Copenhagen, Denmark.
*E-mail address:* thomas.rades@sund.ku.dk (T. Rades).

https://doi.org/10.1016/j.ejpb.2023.04.026
Received 22 February 2023; Received in revised form 28 April 2023; Accepted 29 April 2023
Available online 3 May 2023

the epithelium [4–8].

However, a direct translation from drug dissolution to permeation is sometimes complicated by the complexity of such supersaturating systems, as the apparent concentration of a supersaturated solution is a measure of both molecularly dissolved drug and colloidal drug, e.g. solubilized in micelles, included into cyclodextrins or polymer-bound [5–7,9]. Therefore, drug absorption might be overestimated by the apparent degree of supersaturation if only the concentration gradient of molecularly dissolved drug is driving passive diffusion [8]. A setup combining non-sink dissolution with permeation (D/P-setup) can thus aid in the evaluation of enabling formulations by strictly relying on the molecularly dissolved drug for permeation [8,9]. One approach to such D/P-setups is to incorporate the parallel artificial membrane permeability assay (PAMPA) in which the membrane consists of a hydrophobic polyvinylidene fluoride (PVDF)-filter coated with a phospholipid solution in dodecane [10,11]. PAMPA proved its potential for screening large compound libraries already more than two decades ago by relating PAMPA fluxes to *in vivo* absorption [12]. Since then, several modifications of the PAMPA-barrier have been introduced with alternative barrier supports, membrane composition and/or media composition in donor and receiver compartments, respectively [13]. Yet, without a physical boundary separating the donor compartment and the PAMPA-membrane, its incorporation in a D/P-setup might possess some challenges, e.g. emulsification of phospholipid membrane components into the dissolution medium [13]. While this effect is likely negligible if the amount of phospholipid solution to coat the hydrophobic PVDF-filter is kept at a minimum, another concern could be the risk of drug in suspension directly interacting with the components of the PAMPA-membrane. A plausible result of such interaction with solid particles of a lipophilic drug, e.g. fenofibrate, ritonavir or EFV, could be that direct solubilization in the PAMPA-membrane would contribute to the overall flux and thus an overestimation of drug absorption. Both the PAMPA-, and the alternative phospholipid vesicle-based permeation assay-membrane have previously been modified by incorporating mucus as an additional barrier in a horizontal setup [14,15]. Yet, to the best of our knowledge, the effect on *in vitro-in vivo* relationship by incorporating an additional physical barrier in a vertical D/P-setup allowing for stirring in both donor- and receiver compartment has not been reported before.

Therefore, the first aim of the present study was to investigate whether a PAMPA-based D/P-setup might lack predictability due to the absence of a physical boundary between the PAMPA-membrane and the donor compartment. Secondly, the aim was to investigate if the incorporation of such a physical boundary could successfully improve the *in vivo* predictability of the D/P-setup. Binary polymer based ASDs of the antiretroviral biopharmaceutics classification system class II drug, EFV, were prepared for the evaluation using vacuum compression molding (VCM) as this small-scale preparation procedure had already been established in previous studies [16,17].

## 2. Experimental section

### 2.1. Materials

Efavirenz (EFV) was purchased from Jianbei Pharmaceutical (Zhejiang, China). Two grades of hypromellose acetate succinate (HPMCAS) (Shin-Etsu AQOAT® AS-LF and -MF) were supplied by Shin-Etsu Chemical (Tokyo, Japan). Polyvinyl alcohol (PVOH, GOHSENOL™ EG-03PW) was supplied by Harke Pharma (Mülheim a. d. Ruhr, Germany). Polyvinylpyrrolidone vinylacetate (PVPVA64, Kollidon® VA64) was donated by BASF (Ludwigshafen, Germany). PAMPA-membranes were prepared with hydrophobic polyvinylidene fluoride (PVDF) filters with a pore size of 0.45 μm from Frisenette (Knebel, Denmark) impregnated with gastrointestinal tract (GIT) lipid from Pion Inc. (Billerica, MA, USA). Sodium lauryl sulfate (SLS) and 4-(2-hydroxyethyl)piperazine-1-ethanesulfonic acid (HEPES) were purchased from Sigma-Aldrich (St. Louis, MO, USA) and Hank's Balanced Salt Solution (HBSS, 10x) was acquired from Thermo-Fisher (Waltham, MA, USA).

### 2.2. Preparation and characterization of test formulations

Four ASDs with 20% (*w/w*) EFV in either PVOH, HPMCAS AS-LF, HPMCAS AS-MF or PVPVA64 were prepared for both *in vitro* and *in vivo* assessment. A total amount of 1 g of EFV and polymer was initially mixed in a 25 mL stainless steel jar with two 12 mm stainless steel balls at 30 Hz for 5 min using an oscillatory ball Mixer Mill MM400 from Retsch (Haan, Germany). Approximately 200 mg of the powder mixtures were then molded to ASD discs (ø

20 mm) using a VCM from MeltPrep (Graz, Austria) by heating for 5 min at either 180 °C (PVOH) or at 160 °C (HPMCAS AS-LF, HPMCAS AS-MF and PVPVA64) followed by cooling. Lastly, the ASD discs were processed by short cycles of particle size reduction and sieving to collect a particle size fraction for reproducible testing. This was carried out in 5 mL stainless steel jars with two 5 mm stainless steel balls at 30 Hz using an oscillatory ball Mixer Mill MM400 from Retsch (Haan, Germany) followed by sieving (180–355 μm). An amount of 15–17 mg of the crushed ASD was loaded into size 9 gelatin capsules (Torpac Inc., Fairfield, NJ, USA) for both *in vitro* and *in vivo* assessment. Capsules loaded with an equivalent amount of neat crystalline EFV of 3.0–3.4 mg were also prepared by size fractioning (180–355 μm) quench-cooled EFV followed by storage at 50 °C for 4 days to promote recrystallization. The amorphous nature of the prepared ASDs and the crystallinity of the size fractioned EFV were confirmed by X-ray powder diffraction (XRPD) using an X'Pert PRO X-ray powder diffractometer equipped with a PIXcel detector from PANalytical (Almelo, The Netherlands). Diffractograms were collected using the X'Pert Data Collector software (version 2.2i) from 5 to 30 °2θ using a CuKα radiation source (45 kV, 40 mA, $\lambda = 1.54187$ Å) with a step size of 0.026 °2θ and a scan speed of 0.067 °2θ/s. Scanning electron microscopy (SEM) performed with a TM3030 Tabletop microscope from Hitachi (Tokyo, Japan) was used with an accelerating voltage at 15 kV to evaluate the morphology of the test formulations after particle size fractioning. The samples were gold sputter coated to improve resolution of the SEM using a sputter coater 108auto from Cressington Scientific Instruments (Watford, UK).

### 2.3. In vivo pharmacokinetic study

Male Sprague–Dawley rats (Janvier Labs, Le Genest-Saint-Isle, France) were housed in groups of five or six per cage and allowed to acclimatize for at least one week with a reversed 12/12 h day/night cycle. Fasting of the rats was initiated 12–16 h prior to the studies, with *ad libitum* access to water. The rats were 6–7 weeks old and weighed 270 ± 17 g ($n = 27$) on the day of the studies. The experiments were carried out in agreement with the Danish law on animal experiments as approved by the Danish Animal Experiments Inspectorate in accordance with the EU directive 2010/63/EU under license number 2019–15-0201–00262. The study was designed with five groups receiving an EFV dose of 11.6 ± 0.9 mg/kg by oral gavage of either neat crystalline EFV or a 20% *(w/w)* EFV ASD in size 9 gelatine capsules. Blood samples of 250 μL were drawn from the tail vein into Microvette® 200 K3E tubes (Sarstedt, Nümbrecht, Germany) at 0.5, 1, 2, 3, 4, 6 and 8 h after which a gradient of $CO_2$ gassing was used to kill the rats. The blood plasma was isolated by centrifugation at 9300 × *g* for 10 min at 4 °C in a Microcentrifuge 5415 R (Eppendorf, Hamburg, Germany) and stored at −20 °C until EFV quantification was carried out by high-performance liquid chromatography (HPLC). The plasma samples were prepared for analysis by the addition of an equivalent volume of acetonitrile followed by 5 s of vortexing and storage at 4 °C for 30 min to precipitate the majority of plasma proteins. The precipitated samples were then centrifuged at 9300 × *g* for 10 min at 4 °C in a Microcentrifuge 5415 R (Eppendorf, Hamburg, Germany), and the supernatant analysed by HPLC on a Dionex Ultimate 3000 system (Thermo Fisher Scientific,

Waltham, MA, USA) equipped with a 150 × 2.1 mm ACE Excel 5 C18 column (Advanced Chromatography Technologies, Aberdeen, UK). An isocratic mobile phase of water:acetonitrile (1:1 *v/v*) was applied with a flow rate of 0.6 mL/min resulting in a retention time of EFV of 5.1 min which was quantified as the area under the curve (AUC) of the UV-absorbance at 248 nm (LOQ = 40 ng/mL). A standard curve with $R^2 > 0.999$ was prepared using EFV solutions in ACN (40 – 800 ng/mL) which were mixed 1:1 (*v/v*) with blank plasma followed by identical sample treatment as for the *in vivo* PK samples. All data were further normalized to the EFV dose (mg/kg) administered to each rat.

### 2.4. In vitro Dissolution-Permeation studies

Two dissolution-permeation setups were investigated for potential IVIVR only differentiated by the composition of the barrier between the donor- and receiver compartments. Both setups were based on the MicroFLUX™ model from Pion Inc. (Billerica, MA, USA), allowing for *in situ* concentration monitoring in two compartments of approx. 20 mL separated by a horizontal barrier with an absorptive area of 1.0 $cm^2$ [9,11]. The barrier of the first D/P-setup comprised only of a PAMPA-membrane prepared by the addition of 25 µL GIT-lipid to a hydrophobic PVDF filter (0.45 µm). For the second D/P-setup, an additional filter (hydrophilic PVDF, 0.45 µm) was introduced to act as a physical boundary between the PAMPA-membrane and the donor compartment. The hydrophilic PVDF-filter was gently wetted with a few drops of water and then placed on top of the lipid-coated PAMPA-membrane while making sure that no air bubbles were trapped in between. All other parameters were identical between the two D/P-setups which were initiated by addition of capsule test formulations to the donor compartment identical to the ones used in the *in vivo* PK study. Thereby, the *in vitro* D/P-setups incorporated both the aspect of capsule disintegration while introducing the same EFV amount (3.0–3.4 mg) as was done *in vivo*. The initial 15 min of the studies were carried out with 14.0 mL of diluted HCl (pH 3.5) with 0.2% *(w/w)* NaCl in the donor compartment to mimic the gastric pH as previously measured in rats [18,19]. The intestinal phase was then initiated by the addition of 7.0 mL phosphate buffer (87 mM, pH 7.0) with 1.5% *(w/w)* NaCl resulting in a donor compartment of 21.0 mL phosphate buffer (29 mM, pH 7.0). The receiver compartment was filled with 20.0 mL of acceptor sink buffer (ASB) comprised of 1% *(w/w)* SLS in 10 mM HEPES-buffered HBSS with pH 7.4. Probe tips with a path length of 10 and 20 mm were used for the donor- and receiver compartments, respectively. Standard curves were prepared before each study by the stepwise addition of EFV stock solutions in DMSO not exceeding a final DMSO concentration of 1% *(v/v)*. The maximum concentration range of the standard curve in the donor compartment was limited to 35 µg/mL as immediate precipitation was observed above this concentration. Due to the relatively low concentrations expected in the receiver compartment, a standard curve from 0 to 10 µg/mL was implemented in order to accurately distinguish small differences in this concentration range. A representative example of the obtained spectra and standard curve in the receiver compartment can be found in the supplementary material (Figure S1). Fresh media were then equilibrated to 37 °C with cross magnetic stirrer bars at 250 rpm before initiating the study by the addition of a test formulation in the donor compartment. Concentrations were calculated with the Au PRO Software version 5.5 (Pion Inc, Billerica, MA, USA) based on the UV-absorption at 296 nm and scatter modelling baseline correction at 340 nm.

### 2.5. Visualization of drug particles in contact with the two barrier types

Microscopic visualization of potential dissolution of drug particles in contact with the two barrier types was carried out using an oCelloScope™ System (BioSense Solutions, Farum, Denmark). Circular pieces (ø = 10 mm) of hydrophobic PVDF-filters (0.45 µm) were placed on the bottom of the wells in a 48-well plate and prepared as PAMPA-membranes by the addition of GIT-lipid. One of the membranes was then covered with a wetted piece of hydrophilic PVDF-filter similarly to the conditions of the D/P-setup in which a physical boundary is included between the PAMPA-membrane and the donor compartment. A suspension of crystalline EFV in phosphate buffer (29 mM, pH 7.0) was added in both wells immediately before initiating a 30 min scan of the barrier surfaces. The collected images were analyzed using the background corrected absorption (BCA) algorithm in the UniExplorer software ver. 8.1.

### 2.6. Data analysis

Data were processed with Microsoft Excel 2019 (Redmond, WA, USA) and OriginPro 2020 by OriginLab Corp. (Northampton, MA, USA) or GraphPad Prism version 9 (San Diego, CA, USA) with data expressed as the mean ± standard deviation (SD) unless otherwise stated.

## 3. Results

### 3.1. Preparation and characterization of test formulations

The drug in all four ASDs was confirmed to be amorphous as seen by the absence of reflections corresponding to crystalline forms of the drug (Fig. 1). Fully amorphous ASDs were formed except in the case of PVOH, which showed distinctive peaks due to its semi-crystallinity similar to what has been reported elsewhere [20]. Furthermore, recrystallization of the size fractioned EFV particles was confirmed, as distinctive peaks corresponding to the EFV polymorph I [21] were observed in the diffractogram (Fig. 1).

The ASD particle size reduction was achieved by ball milling which caused a plausible risk that the collected size fraction (180–355 µm) would partly consist of agglomerated smaller particles. Therefore, images of the particle morphology were acquired by SEM (Fig. 2) which confirmed that the collected ASD particles were indeed single particles with smooth surfaces. Recrystallization of the neat EFV particles upon storage at 50 °C was also evident by SEM, as the surface of recrystallized neat EFV can be seen covered with crystals (Fig. 2A-C) in contrast to the smooth surface of the HPMCAS AS-LF-based ASD (Fig. 2D-F). Additional SEM images of all the formulations can be found in the supplementary material (Figure S2).

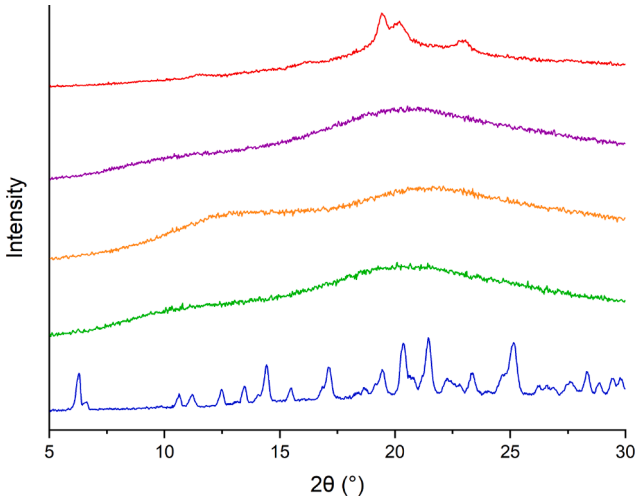


**Fig. 1.** Normalized X-ray powder diffractograms of the four amorphous solid dispersions (ASDs) of efavirenz (EFV) (20% w/w) in polyvinyl alcohol (PVOH, red), hypromellose acetate succinate AS-MF (HPMCAS AS-MF, purple), polyvinylpyrrolidone vinylacetate (PVPVA64, orange), HPMCAS AS-LF (green) and of recrystallized EFV (blue). (For interpretation of the references to colour in this figure legend, the reader is referred to the web version of this article.)

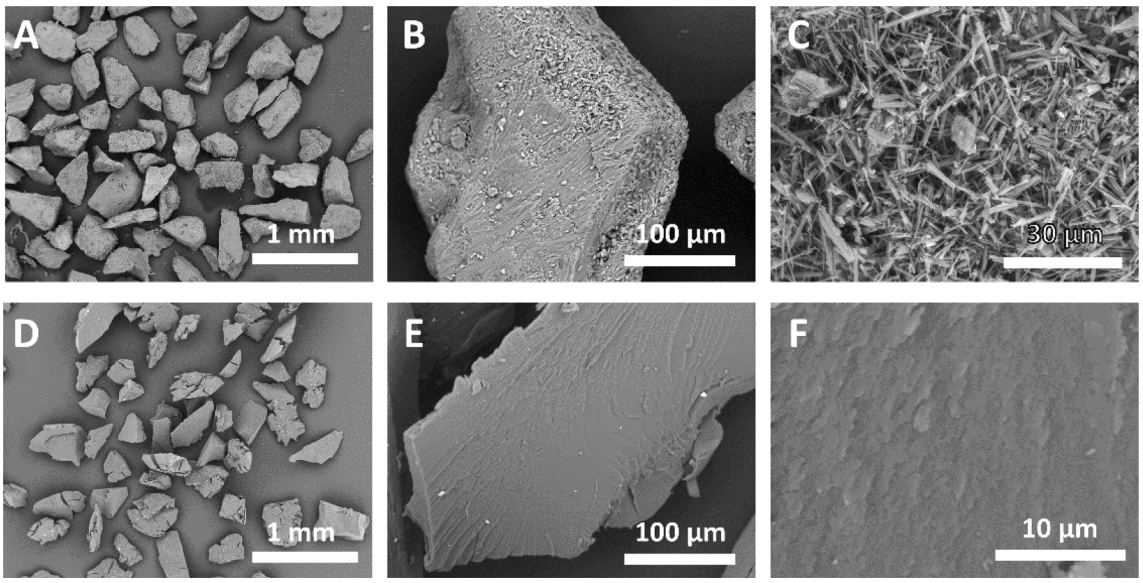


**Fig. 2.** Scanning electron micrographs of two of the test formulations after particle size fractioning (180–355 µm). ***A-C:*** Neat recrystallized EFV particles after four days of storage at 50 °C. ***D-F*** ASD of 20% *(w/w)* EFV in HPMCAS AS-LF.

### 3.2. *In vivo pharmacokinetic study*

The plasma concentration profiles of EFV after oral gavage of the test formulations to rats are shown in Fig. 3.

All four ASDs showed similar PK profiles with comparable pharmacokinetic parameters ($C_{max}$, $T_{max}$ and AUC) as listed in Table 1. The only significant difference observed between the ASDs was that of the AUCs between the PVPVA64 (1250 ± 262 h·ng/mL) and the HPMCAS AS-MF-based ASD (1673 ± 236 h·ng/mL). Yet, all ASDs had significantly higher $C_{max}$ and AUCs compared to neat crystalline EFV with mean AUCs in the order

HPMCAS AS-MF > PVOH > HPMCAS AS-LF > PVPVA64.

### 3.3. *In vitro Dissolution-Permeation studies*

The five test formulations were tested in two *in vitro* D/P-setups both based on *in situ* concentration monitoring in the MicroFLUX™ apparatus from Pion Inc. (Billerica, MA, USA) with the only difference being the type of permeation barrier installed. The first D/P-setup based on the PAMPA-membrane alone showed significant discrepancies between the EFV dissolution profiles in the donor compartment and the EFV permeation profiles in the receiver compartment (Fig. 4).

While the PVOH-based ASD maintained an apparent concentration

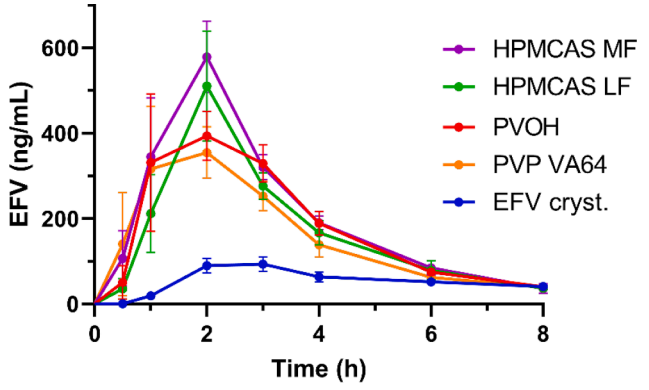


**Fig. 3.** Pharmacokinetic profiles of EFV following oral administration of neat crystalline EFV and four ASDs of 20% (*w/w*) EFV in the listed polymer matrices. Data presented as mean ± standard error of the mean (SEM), ($n$ = 5–6).

**Table 1**
Pharmacokinetic parameters of EFV following oral administration of neat crystalline EFV ($EFV_{cryst}$) and four ASDs of 20% (*w/w*) EFV in the listed polymer matrices. Data presented as mean ± SD.

| | HPMCAS AS-MF | HPMCAS AS-LF | PVOH | PVPVA64 | $EFV_{cryst}$ |
|---|---|---|---|---|---|
| $C_{max}$ (ng/mL) | 601 ± 182[b] | 540 ± 241[a] | 508 ± 250[a] | 476 ± 271[a] | 108 ± 32 |
| $T_{max}$ (h) | 1.8 ± 0.4 | 2.2 ± 0.4 | 2.4 ± 0.9 | 1.8 ± 0.8 | 3.2 ± 1.5 |
| $AUC_{0\text{-}8h}$ (h·ng/mL) | 1673 ± 236[*,c] | 1396 ± 259[c] | 1454 ± 244[c] | 1250 ± 260[*,c] | 435 ± 63 |

Values indicated with an upper asterisk (*) are significantly different ($P < 0.05$), while values indicated with a letter ([a] $P < 0.05$, [b] $P < 0.01$, [c] $< 0.0001$) are significantly different to the corresponding values of $EFV_{cryst.}$ (ANOVA with Tukey's multiple comparison test).

in the donor compartment of 4–5 times that of both the PVPVA64-based ASD and neat crystalline EFV, their respective EFV permeation profiles were basically identical. This immediately suggested room for improvement of the D/P-setup as the *in vivo* PK study resulted in significantly lower AUC and $C_{max}$ from the neat crystalline EFV compared to all the ASDs (Table 1). A 100% solubilization in the donor compartment would correspond to an EFV concentration of 152 µg/mL based on a dose of 3.2 mg in the intestinal buffer of 21 mL. Thus, with a donor concentration plateauing at the equilibrium solubility of 12 µg/mL after dosing neat crystalline EFV, <10% of the drug was dissolved. Ideally, this should not contribute to the flux of EFV other than maintaining the free drug concentration gradient by continues dissolution as a result of permeation. Yet, the neat crystalline EFV led to the same amount of drug permeation as the PVOH- and PVPVA64-based ASDs which potentially could be a result of solubilization of EFV particles in the phospholipid-dodecane solution of the PAMPA-membrane. The permeation barrier was therefore modified in a second *in vitro* setup, such that a hydrophilic PVDF-filter was incorporated facing the donor compartment to reduce the potential of direct interaction between solid EFV particles and the PAMPA-membrane. The concentration profiles of the second *in vitro* D/P-setup are shown in Fig. 5.

As expected, the dissolution profiles in the second D/P-setup were similar to those observed in the first D/P-setup, as the modification was

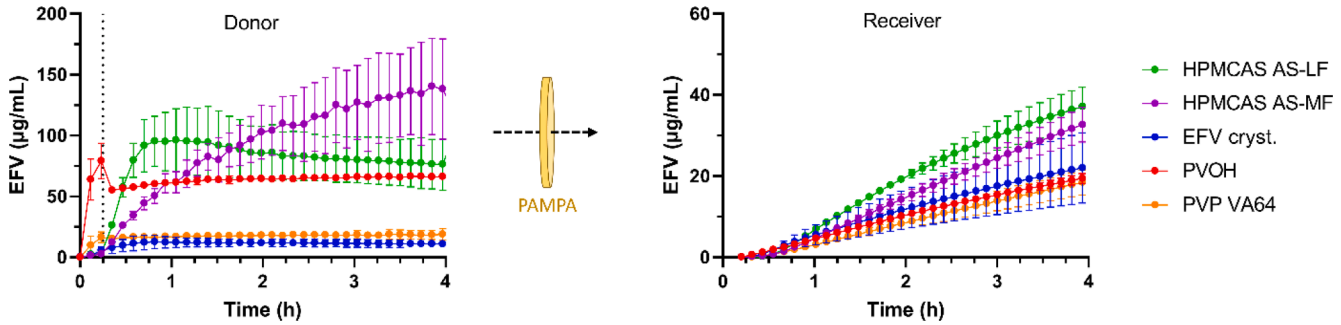


**Fig. 4.** EFV concentration profiles in the donor and receiver compartments of the *in vitro* dissolution-permeation (D/P) setup with PAMPA-membrane alone as the permeation barrier. The test formulations (neat crystalline EFV and four ASDs of 20% (*w/w*) EFV in the listed polymer matrices in size 9 gelatin capsules) were added to the donor compartment at t = 0 min. The dotted line on the left graph indicates the change from gastric pH 3.5 to intestinal pH 7.0. Data presented as mean ± SD, ($n$ = 3–4).

strictly confined to the barrier. Nevertheless, the addition of the hydrophilic PVDF-filter dramatically changed the EFV concentration measured in the receiver compartment. In general, a 10-fold reduction of the receiver EFV concentrations was observed in the D/P-setup including the hydrophilic boundary compared to the D/P-setup only applying a PAMPA-membrane. In terms of rank order of the formulations, the most notable difference was a relative drop in the performance of the neat crystalline EFV together with an improvement of its reproducibility. Another significant change was observed for the HPMCAS AS-LF based ASD which out-performed the other formulations when only the PAMPA-membrane was installed. Yet, with the additional PVDF-filter, both HPMCAS-based ASDs had very similar receiver concentration profiles.

### 3.4. In Vitro-In vivo relationship

The predictabilities of the two D/P-setups were evaluated based on linear regressions when plotting the full 8 h *in vivo* AUCs against the AUCs of the initial 2.5 h of the receiver concentrations as shown in Fig. 6. The 2.5 h *in vitro* AUC was chosen as this allowed for including *in vitro* data for 2 h excluding the initial lag-phase in the receiver compartments. Furthermore, the IVIVR did not improve from extending the *in vitro* AUC to 3 or 4 h as shown in Figure S3.

No correlation was observed between the AUCs of the EFV plasma profiles from the PK study and the AUCs of the receiver compartment from the D/P-setup when the barrier only consisted of the PAMPA-membrane. However, a similar plot based on *in vitro* data from the D/P-setup with the additional hydrophilic PVDF-filter resulted in a linear correlation ($R^2 = 0.97$). The improvement in IVIVR when incorporating the hydrophilic PVDF-filter was primarily driven by the drop in the *in vitro* performance of neat crystalline EFV and the ASD based on HPMCAS AS-LF relative to the other ASDs. The two barrier types were further investigated microscopically to elucidate whether this dramatic improvement of the D/P-setup could be due to the effect of the additional hydrophilic PVDF-filter blocking crystalline drug particles from interacting with the PAMPA-membrane.

### 3.5. Visualization of drug particles in contact with the barrier types

The two barrier types were immersed in a crystalline suspension of EFV and the barrier surfaces monitored using the oCelloScope™ System (BioSense Solutions, Farum, Denmark). The relative barrier surface area being covered with EFV particles is shown in Fig. 7, plotted as normalized BCA over time after the addition of the crystalline suspension of EFV.

The images acquired on the surface of the hydrophilic PVDF filter placed on top of the PAMPA-membrane were distorted due to significantly reduced light transmission making the images appear black. Nevertheless, the BCA algorithm was able to correct the background intensity in order to track sedimentation of EFV particles on the barrier surface reaching a maximum BCA after about 20 min. On the other hand, images through the PAMPA barrier resulted in well illuminated images, thus making it possible to relate the calculated BCA to the visual evidence of the EFV particle distribution on the barrier surface (video can be found in the supplementary material). The EFV particle density reached a maximum on the PAMPA barrier after about 5 min after which a gradual decline is observed most likely caused by EFV dissolution in the PAMPA-membrane components.

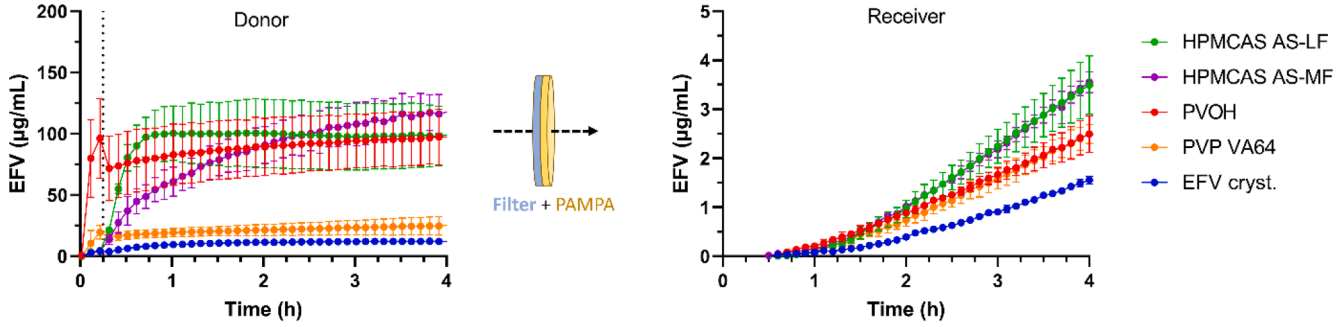


**Fig. 5.** EFV concentration profiles in the donor and receiver compartments of the *in vitro* D/P-setup incl. a hydrophilic PVDF-filter as physical boundary between the PAMPA-membrane and the donor compartment. The test formulations (neat crystalline EFV and four ASDs of 20% (*w/w*) EFV in the listed polymer matrices in size 9 gelatin capsules) were added to the donor compartment at t = 0 min. The dotted line on the left graph indicates the change from gastric pH 3.5 to intestinal pH 7.0. Data presented as mean ± SD, ($n$ = 3–4).

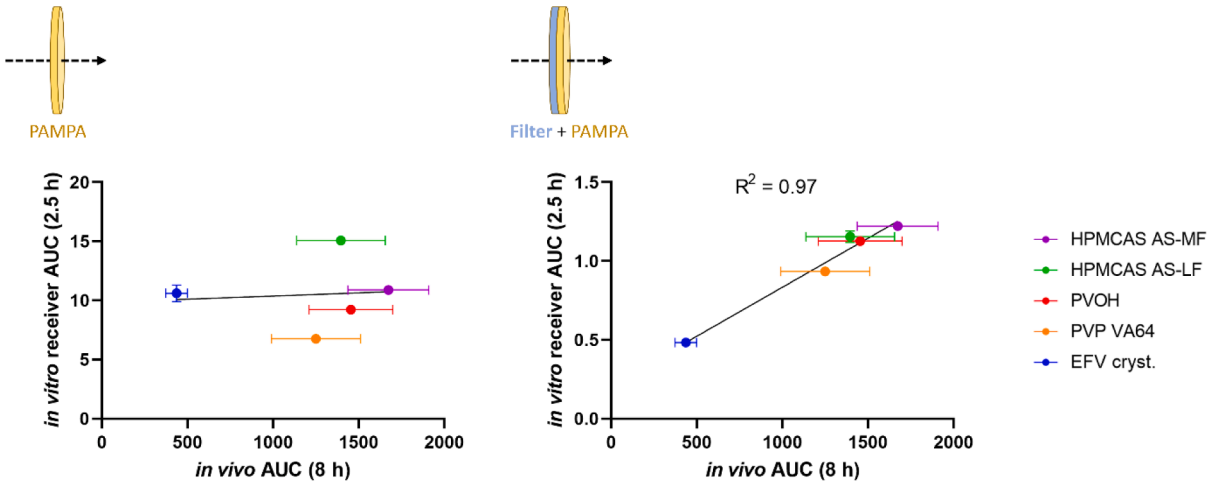


**Fig. 6.** Area under the curves (AUCs) of EFV receiver concentrations of the initial 2.5 h of the two *in vitro* D/P-setups as a function of the full 8 h AUCs of the EFV pharmacokinetic profiles in rats. The five test formulations were neat crystalline EFV and four ASDs of 20% (*w/w*) EFV in the listed polymer matrices. ***Left:*** *In vitro* data from the D/P-setup only with a PAMPA-membrane as barrier. ***Right:*** *In vitro* data from the D/P-setup with the additional hydrophilic PVDF-filter as physical boundary between the PAMPA-membrane and the donor compartment. Data presented as mean ± SD, ($n$ = 3–6). Some error bars do not appear as they are shorter than the size of the symbol.

## 4. Discussion

The predictability of an *in vitro* setup depends on its capability to distinguish absorbable drug species, i.e. molecularly dissolved, from nonabsorbable species, e.g. solubilized in micelles, polymer-bound or even solid particles. The current findings of EFV suggest that a D/P-setup with only a PAMPA-membrane as barrier might lack predictability, due to potential dissolution of solid drug particles in the membrane components. In the present study, we decided to test this hypothesis with crystalline EFV and binary ASD formulations (amorphization confirmed by XRPD), all dosed with a fixed EFV amount and particle size fraction (confirmed by SEM). The average flux and the variability observed from neat crystalline EFV was relatively high compared to the four ASDs when using the PAMPA-membrane alone as barrier in the D/P-setup. A possible explanation for this high variability of the flux could be that it not only depends on the equilibrium solubility in the donor compartment, but also on the amount of EFV particles that by chance come in direct contact with the PAMPA-membrane on the donor side. Being a relatively lipophilic drug (logP ≈ 4) [22], such direct contact might not surprisingly result in dissolution in the phospholipid-dodecane mixture of the membrane as observed in the microscopic visualization. In contrast, with the addition of the hydrophilic PVDF-filter as a physical boundary between PAMPA-membrane and the donor compartment, such solubilization at the barrier surface was not observed and neither was the overperformance nor the variability of the neat crystalline EFV compared to the ASDs. Thus, the additional boundary can be regarded to act as a simple analogue to the mucus layer, which likewise acts as the physical but far more complex and dynamic boundary between luminal content and the epithelial tissue *in vivo* [23]. The negative charge of mucus might to some extend be featured by the addition of a PVDF filter [24], however dur to its simplicity, it will inevitably fail to recreate the interactive properties of endogenous mucus. Mucus has previously been incorporated in artificial membrane-based *in vitro* permeation setups, yet these studies have been limited to horizontal barriers [14,15]. In

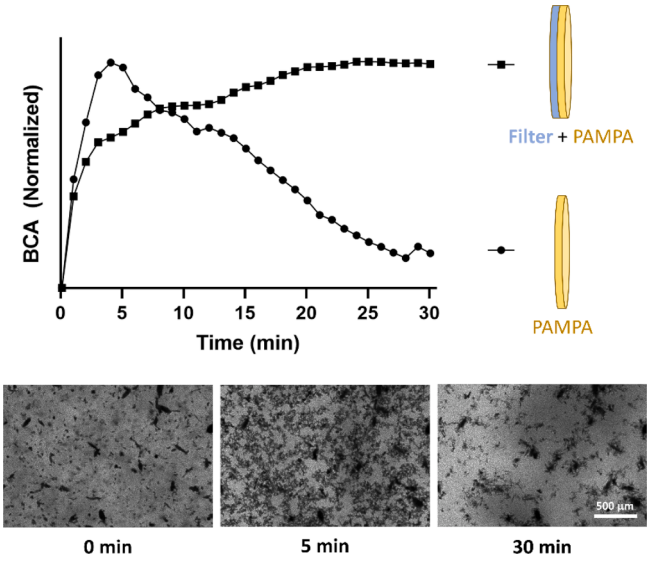


**Fig. 7.** Image analysis of EFV particle distribution on the two barrier types. ***Top:*** Normalized background corrected absorption (BCA) analysis. ***Bottom*** Images of EFV particle distribution on the surface of the PAMPA-membrane after 0, 5 and 30 min.

contrast, the present PVDF-filter has the advantage of also being compatible with vertical barriers, e.g. the PAMPA membrane of the microFLUX® setup. However, whether this additional physical boundary is necessary in order to achieve IVIVR might depend on the test formulations and/or the physicochemical properties of the drug. There is a rationale for an additional physical boundary between the donor compartment and the PAMPA-membrane when the drug is either added as a solid formulation or if the drug tends to precipitate during the experiment. Furthermore, it is plausible that its relevance increases with the lipophilicity of the drug as a result of greater affinity to the PAMPA-membrane components.

## 5. Conclusion

The present study successfully established a linear IVIVR ($R^2 = 0.97$) between an *in vitro* D/P-setup and a rat PK study of five test formulations of EFV incl. four ASDs (with HPMCAS AS-LF and -MF, PVOH, PVPVA64 as carrier polymers) and a crystalline formulation. This was achieved by modifying the D/P-setup with the addition of a physical boundary between the donor compartment and the PAMPA-membrane, thereby precluding solid drug particles in suspension from interacting with the lipid components of the PAMPA-membrane. Microscopic visualization supported the hypothesis that such interaction could otherwise result in direct drug dissolution in the lipid components of the PAMPA-membrane and consequently contribute to the overall flux. This potential contribution to the flux might thus in general be a relevant factor to preclude when assessing formulations that are prone to cause precipitation. The relatively easy modification of the barrier by introducing a hydrophilic filter is thereby likely to provide a stronger preclinical foundation in the formulation development of enabling formulations by resulting in a more accurate rank order and estimation of bioavailability improvement.

## CRediT authorship contribution

**Jacob R. Jørgensen:** Conceptualization, Methodology, Investigation, Writing - Original Draft, Visualization. **Wolfgang Mohr:** Conceptualization, Resources, Methodology, Writing - Review & Editing. **Matthias Rischer:** Conceptualization, Resources, Methodology, Writing - Review & Editing. **Andreas Sauer:** Conceptualization, Resources, Methodology, Writing - Review & Editing. **Shilpa Mistry:** Conceptualization, Resources, Methodology, Writing - Review & Editing. **Thomas Rades:** Conceptualization, Resources, Methodology, Writing - Review & Editing. **Anette Müllertz:** Conceptualization, Resources, Methodology, Writing - Review & Editing.

## Declaration of Competing Interest

The authors declare that they have no known competing financial interests or personal relationships that could have appeared to influence the work reported in this paper.

## Data availability

Data will be made available on request.

## Appendix A. Supplementary data

Supplementary data to this article can be found online at https://doi.org/10.1016/j.ejpb.2023.04.026.

## References

[1] F. Thomas, Tackling Solubility in Drug Development, Pharm. Technol. 43 (2019) 24–25.
[2] F. Ditzinger, D.J. Price, A.-R. Ilie, N.J. Köhl, S. Jankovic, G. Tsakiridou, S. Aleandri, L. Kalantzi, R. Holm, A. Nair, C. Saal, B. Griffin, M. Kuentz, Lipophilicity and hydrophobicity considerations in bio-enabling oral formulations approaches – a PEARRL review, J. Pharm. Pharmacol. 71 (2019) 464–482, https://doi.org/10.1111/jphp.12984.
[3] S. Kalepu, M. Manthina, V. Padavala, Oral lipid-based drug delivery systems – an overview, Acta Pharm. Sin. B. 3 (2013) 361–372, https://doi.org/10.1016/j.apsb.2013.10.001.
[4] P. Pandi, R. Bulusu, N. Kommineni, W. Khan, M. Singh, Amorphous solid dispersions: An update for preparation, characterization, mechanism on bioavailability, stability, regulatory considerations and marketed products, Int. J. Pharm. 586 (2020) 119560, https://doi.org/10.1016/j.ijpharm.2020.119560.
[5] L.S. Taylor, G.G.Z. Zhang, Physical chemistry of supersaturated solutions and implications for oral absorption, Adv. Drug Deliv. Rev. 101 (2016) 122–142, https://doi.org/10.1016/j.addr.2016.03.006.
[6] A. Schittny, J. Huwyler, M. Puchkov, Mechanisms of increased bioavailability through amorphous solid dispersions: A review, Drug Deliv. 27 (2020) 110–127, https://doi.org/10.1080/10717544.2019.1704940.
[7] A. Newman, G. Knipp, G. Zografi, Assessing the performance of amorphous solid dispersions, J. Pharm. Sci. 101 (2012) 1355–1377, https://doi.org/10.1002/jps.23031.
[8] S.T. Buckley, K.J. Frank, G. Fricker, M. Brandl, Biopharmaceutical classification of poorly soluble drugs with respect to "enabling formulations", Eur. J. Pharm. Sci. 50 (2013) 8–16, https://doi.org/10.1016/j.ejps.2013.04.002.
[9] C. Alvebratt, J. Keemink, K. Edueng, O. Cheung, M. Strømme, C.A.S. Bergström, An in vitro dissolution–digestion–permeation assay for the study of advanced drug delivery systems, Eur. J. Pharm. Biopharm. 149 (2020) 21–29, https://doi.org/10.1016/j.ejpb.2020.01.010.
[10] K.A. Lentz, J. Plum, B. Steffansen, P.-O. Arvidsson, D.H. Omkvist, A.J. Pedersen, C. J. Sennbro, G.P. Pedersen, J. Jacobsen, Predicting in vivo performance of fenofibrate amorphous solid dispersions using in vitro non-sink dissolution and dissolution permeation setup, Int. J. Pharm. 610 (2021) 121174, https://doi.org/10.1016/j.ijpharm.2021.121174.
[11] J.N. Eliasen, R. Berthelsen, A.L. Slot, A. Müllertz, Evaluating side-by-side diffusion models for studying drug supersaturation in an absorptive environment: A case example of fenofibrate and felodipine, J. Pharm. Pharmacol. 72 (2020) 371–384, https://doi.org/10.1111/jphp.13218.
[12] M. Kansy, F. Senner, K. Gubernator, Physicochemical High Throughput Screening: Parallel Artificial Membrane Permeation Assay in the Description of Passive Absorption Processes, J. Med. Chem. 41 (1998) 1007–1010, https://doi.org/10.1021/jm970530e.
[13] P. Berben, A. Bauer-Brandl, M. Brandl, B. Faller, G.E. Flaten, A.-C. Jacobsen, J. Brouwers, P. Augustijns, Drug permeability profiling using cell-free permeation tools: Overview and applications, Eur. J. Pharm. Sci. 119 (2018) 219–233, https://doi.org/10.1016/j.ejps.2018.04.016.
[14] M. Falavigna, M. Klitgaard, C. Brase, S. Ternullo, N. Škalko-Basnet, G.E. Flaten, Mucus-PVPA (mucus Phospholipid Vesicle-based Permeation Assay): An artificial permeability tool for drug screening and formulation development, Int. J. Pharm. 537 (2018) 213–222, https://doi.org/10.1016/j.ijpharm.2017.12.038.
[15] C. Butnarasu, G. Caron, D.P. Pacheco, P. Petrini, S. Visentin, Cystic Fibrosis Mucus Model to Design More Efficient Drug Therapies, Mol. Pharm. 19 (2022) 520–531, https://doi.org/10.1021/acs.molpharmaceut.1c00644.
[16] J.R. Jørgensen, W. Mohr, M. Rischer, A. Sauer, S. Mistry, A. Müllertz, T. Rades, Stability and intrinsic dissolution of vacuum compression molded amorphous solid dispersions of efavirenz, Int. J. Pharm. 632 (2023) 122564, https://doi.org/10.1016/j.ijpharm.2022.122564.
[17] G. Shadambikar, T. Kipping, N. Di-Gallo, A.-G. Elia, A.-N. Knüttel, D. Treffer, M. A. Repka, Vacuum Compression Molding as a Screening Tool to Investigate Carrier Suitability for Hot-Melt Extrusion Formulations, Pharmaceutics. 12 (2020) 1019, https://doi.org/10.3390/pharmaceutics12111019.
[18] J.F. Christfort, S. Strindberg, J. Plum, J. Hall-Andersen, C. Janfelt, L.H. Nielsen, A. Müllertz, Developing a predictive *in vitro* dissolution model based on gastrointestinal fluid characterisation in rats, Eur. J. Pharm. Biopharm. 142 (2019) 307–314, https://doi.org/10.1016/j.ejpb.2019.07.007.
[19] E.L. McConnell, A.W. Basit, S. Murdan, Measurements of rat and mouse gastrointestinal pH, fluid and lymphoid tissue, and implications for in-vivo experiments, J. Pharm. Pharmacol. 60 (2008) 63–70, https://doi.org/10.1211/jpp.60.1.0008.
[20] J. Macedo, A. Samaro, V. Vanhoorne, C. Vervaet, J.F. Pinto, Processability of poly (vinyl alcohol) Based Filaments With Paracetamol Prepared by Hot-Melt Extrusion for Additive Manufacturing, J. Pharm. Sci. 109 (2020) 3636–3644, https://doi.org/10.1016/j.xphs.2020.09.016.
[21] C. Fandaruff, G.S. Rauber, A.M. Araya-Sibaja, R.N. Pereira, C.E.M. de Campos, H.V. A. Rocha, G.A. Monti, T. Malaspina, M.A.S. Silva, S.L. Cuffini, Polymorphism of Anti-HIV Drug Efavirenz: Investigations on Thermodynamic and Dissolution Properties, Cryst. Growth Des. 14 (2014) 4968–4975, https://doi.org/10.1021/cg500509c.
[22] J.H. Fagerberg, E. Karlsson, J. Ulander, G. Hanisch, C.A.S. Bergström, Computational Prediction of Drug Solubility in Fasted Simulated and Aspirated Human Intestinal Fluid, Pharm. Res. 32 (2015) 578–589, https://doi.org/10.1007/s11095-014-1487-z.
[23] M. Boegh, H.M. Nielsen, Mucus as a barrier to drug delivery – Understanding and mimicking the barrier properties, Basic Clin. Pharmacol. Toxicol. 116 (2015) 179–186, https://doi.org/10.1111/bcpt.12342.
[24] J. Guo, M.U. Farid, E.-J. Lee, D.-Y.-S. Yan, S. Jeong, A. Kyoungjin An, Fouling behavior of negatively charged PVDF membrane in membrane distillation for removal of antibiotics from wastewater, J. Membr. Sci. 551 (2018) 12–19, https://doi.org/10.1016/j.memsci.2018.01.016.